Real-Time Measurement of Fluorescence Spectra from Single Airborne Biological Particles

Steven C. Hill,[1] Ronald G. Pinnick,[1] Stanley Niles,[1] Yong-Le Pan,[2] Stephen Holler,[3] Richard K. Chang,[3] Jerold Bottiger,[4] Bean T. Chen,[5] Chun-Sing Orr,[5] and Greg Feather[5]

[1]*U. S. Army Research Laboratory, 2800 Powder Mill Road, Adelphi, Maryland 20783*

[2]*Physical Sciences Laboratory, New Mexico State University, Las Cruces, New Mexico 88003*

[3]*Applied Physics, Yale University, New Haven, Connecticut 06520*

[4]*U. S. Army Edgewood Chemical and Biological Center, Aberdeen Proving Ground, Maryland 21010*

[5]*National Institute of Occupational Safety and Health, Morgantown, West Virginia 26505*

Received 10 May 1999; revised 14 July 1999; accepted 22 July 1999

Abstract: Improved real-time methods for characterizing airborne biological particles are needed. Here we review our efforts in developing techniques for measuring the laser-induced fluorescence (total and spectrally dispersed) of individual airborne particles, and describe our present system, which can measure fluorescence spectra of single micrometer-sized bioaerosol particles with good signal-to-noise ratios. We demonstrate the capability of this system by showing measured spectra of a variety of airborne particles generated in the laboratory from road dust, ammonium sulfate, *Bacillus subtilis* and other bacteria prepared under various conditions, allergens, cigarette smoke, and chicken-house dust. These spectra illustrate the capability of the system to distinguish *between* some biological and nonbiological aerosols, and *among* several types of laboratory-generated biological aerosols. We suggest improvements needed to make our system field portable. © 1999 John Wiley & Sons, Inc.* Field Analyt Chem Technol 3: 221–239, 1999

Keywords: bioaerosols; aerosol detection; fluorescence spectroscopy; instrumentation; single-particle fluorescence; biological aerosols

Correspondence to: S. C. Hill

Contract grant sponsor: U. S. Air Force Research Laboratory
Contract grant sponsor: Army Research Laboratory (ARL)
Contract grant number: DAAL01-98-C0056, DAAL01-97-2-0218
Contract grant sponsor: U. S. Army Research Office
Contract grant number: DAAG55-97-1-0349, DAAG-97-1-0199 for (S. Holler

Introduction

The Bioaerosol Detection Problem

Bioaerosols are ubiquitous in the earth's tropospheric boundary layer, although they typically occur in small concentrations.[1–3] They have both natural and anthropogenic sources. Bioaerosols are found in the workplace,[4] in residential houses,[5] in medical facilities,[6,7] in manufacturing operations in which metalworking fluids are used,[8] in animal-hair processing facilities,[9] in dairy facilities,[10] or other animal houses,[11] in sites of sludge application,[12] in recycling or composting plants,[13] in sanitary landfills,[14] and in sewage plants.[15] Unlike most common atmospheric aerosols, airborne microorganisms can cause disease, allergies, and respiratory problems. Bioaerosols are feared as potential biowarfare and terrorist agents.[16–19]

Improved methods for measuring aerosols, particularly bioaerosols, are needed. Presently, methods that measure aerosol size distributions in real time provide almost no information about particle types and are not able to identify specific microorganisms. Efforts to develop field-portable instruments for detection and identification of airborne biological particles have accelerated during the last several years.[20]

The ideal instrument for detecting bioaerosols would be compact and portable, would have a fast response, and would provide specific identification. Current efforts are concentrated on two complementary types of apparatus: (1) a bioaerosol detector that could operate continuously without consumables and give a real-time indication of the presence of bioaerosol particles in certain broad classes, and (2) an identifier of specific microorganisms, based on biological

recognition molecules, which (it now appears) would be slower, would require consumables and a logistics trail, and would require collection of the particles.[21–26] These two types might be combined into a single instrument, with the bioaerosol detector serving as a warning device indicating when to turn on the identifier for specific microorganisms.

A bioaerosol detector that provides real-time detection, even without specific identification of bacteria or protein toxins in particles, would be useful for studying the prevalence and dispersion of bioaerosols in the atmospheric boundary layer, in the workplace, in medical and agricultural facilities, etc. A potential limitation of instruments that identify specific microorganisms in a reasonable time (e.g., 30 min) is that such instruments at present require the prior generation of specific recognition molecules for each microbe, allergen, or toxin of interest. A bioaerosol detector that does not identify might be particularly useful in cases where new or unexpected types of bioaerosol occur. The primary quasi-real-time bioaerosol detection methods that require no reagents and are not capable of identifying specific microorganisms fall into two categories: (1) those that exploit the intrinsic fluorescence (total[27–30] or spectrally dispersed[31–37]) of biological molecules, and (2) those that perform mass spectrometry of ions created by laser ablation,[38] laser desorption,[39–40] or pyrolysis[43–46] of particles.

Intrinsic Fluorescence-Based Bioaerosol Detection

Building a point detector that exploits the intrinsic fluorescence of bioaerosol particles for their detection and classification is technically challenging for several reasons. First, particles of interest may exist as a small concentration in a dominant background. Average fluorescence spectra accumulated for a population of aerosol particles may yield little or no information about the few particles of interest; that is, single-particle spectra are required. Second, fluorescence signals are weak because single particles contain only a few picograms of material, and only a small fraction of the mass of biological particles consists of fluorophors.[47,48] Third, particles are generally dispersed nonuniformly in the air (their concentration fluctuations follow the Kolmogorov spectrum of atmospheric turbulence), and they must be detected at random times as they are carried rapidly by a stream of air through an optical cell. Fourth, an optimal detector should excite particles in the ultraviolet, where most biological particles (and biological molecules) fluoresce efficiently. Ultraviolet laser sources are relatively expensive and have relatively low energy output. Fifth, bioaerosols of interest, including individual particles in bioaerosols, may be complex mixtures. Fluorescence from various components of the mixture may limit the usefulness of classification schemes. If fluorescence emission bands were narrow and the number of possible materials in a single particle were small, then it may be possible to solve the inverse problem and determine the materials that contributed to the spectrum. However, the intrinsic fluorescence bands from biological materials tend to be spectrally wide, the primary fluorophors in the majority of bioaerosols fall into only a few broad categories[49–52] [e.g., the aromatic amino acids, tryptophan, tyrosine, and phenylalanine; nicotinamide adenine dinucleotide compounds (NADH); flavins; and chlorophylls], and the number of possible materials is very large. The differences between spectra of bacteria appear to depend on preparation methods (growth media, type and extent of washing of the samples, etc.) more than they depend on intrinsic variations between well-purified bacteria.[37,53]

Therefore, we are now realizing that it will not be possible, except with severely restricted classes of bioaerosols, to identify specific bioaerosols based only on their fluorescence spectra and their size (as determined from elastic scattering). The extent to which it will be possible to characterize naturally occurring and anthropogenically produced bioaerosols (e.g., group them into a few or even a few tens of categories) is yet unknown. Our goal at this stage is to demonstrate that fluorescence spectra of bioaerosols can be measured in real time, and to show that the single-particle spectra obtained are sufficiently different to suggest that the technique may be a powerful diagnostic tool for bioaerosol classification. Improvements in our technique will be needed for its evolution into a field-portable detector that can be used to study bioaerosols in various atmospheric environments.

Overview

We report here on our recent advances that exploit the intrinsic fluorescence of bioaerosols as a diagnostic for their rapid detection and classification. We briefly review these advances: (1) the development of a fluorescence particle counter for measuring the elastic scattering and undispersed fluorescence [excited with a continuous-wave (cw) 488-nm laser] of individual particles as they are carried by an air stream through an optical cell;[27] (2) the development of a method for measuring the fluorescence spectra of ensembles of airborne particles as they flow through a laser beam;[31] (3) the use of a conditional sampling strategy[32] [with a gateable image-intensified CCD (charge-coupled device) camera] for measuring single-particle fluorescence spectra of individual bioaerosol particles excited with a single cw laser; (4) the introduction of a conditional laser-firing strategy, wherein particles are excited by a pulsed UV laser that is triggered to fire (triggered by scattering signals from a cw laser) when particles traverse the sample volume;[33,34] and (5) the further refinement of the conditional firing technique, the use of a more precise crossed-beam triggering system and large-numerical-aperture reflective optics, which results in a superior capability for rapidly measuring high-quality, UV-excited fluorescence spectra of single micrometer-sized bioaerosol particles as they are carried by a stream of air through an interrogation region.[35,36]

We demonstrate that with our latest technique (1) fluorescence spectra of single particles (which are agglomerates of bacteria) as small as 1.8 μm in diameter can be measured with repeatability; (2) fluorescence spectra of a trace concentration of potentially interesting bioaerosol particles entrained within a dominant concentration of other biological

particles can be measured; (3) fluorescence spectra can be used to differentiate biological particles (e.g., *Bacillus subtilis*) from some common atmospheric aerosol particles (ammonium sulfate, soil-derived particles, black carbon, ammonium nitrate); (4) bacteria (e.g., *B. subtilis*) and some common biological particles can be distinguished from their fluorescence spectra; (5) the same bacteria grown under different conditions can be differentiated based on their fluorescence spectra; (6) fluorescence spectra of washed and unwashed bacterial samples are different; (7) even though the spectra of two samples (fungal spores and *B. subtilis*) are similar when excited at one UV wavelength (266 nm) they can be different when excited at another wavelength (351 nm); (8) conversely, two samples that have similar 351-nm-excited spectra can have different 266-nm-excited spectra, demonstrating that multiwavelength excitation of fluorescence can be a more powerful diagnostic for classifying biological particles compared to single-wavelength excitation; and (9) the 266-nm-excited fluorescence spectra of *B. subtilis* and tobacco smoke are similar (with only subtle differences), suggesting that particle size in combination with spectral measurements may be particularly useful for distinguishing between smoke and bacterial particles (tobacco smoke particles tend to have submicrometer sizes).

Our latest technique represents the culmination of our efforts over the last several years to exploit laser-induced fluorescence to detect and classify bioaerosol particles. The technique has not yet been engineered onto a platform suitable for field applications. However, the availability of diode-pumped solid-state lasers (which we have used here to demonstrate the technique), advances in UV semiconductor lasers, and advances in multianode PMT detectors should make a field-portable system practical.

Development of the Fluorescence Particle Counter and the Spectrometer

Fluorescence Particle Counter (FPC)

In our first attempt[27] to measure the fluorescence of single bioaerosol particles we constructed an optical cell to measure the elastic scattering and fluorescence of single particles as they were carried by an air stream through the cell (we modified a cell used in a light-scattering aerosol counter available commercially from Particle Measuring Systems, Inc., Boulder, CO). Particles were illuminated with a cw argon-ion laser, either 0.7 kW/cm^2 extracavity or 50 kW/cm^2 intracavity at 488-nm wavelength. Although fluorescence in flavins is excited at this wavelength, fluorescence of amino acids and NADH is not. To increase sensitivity, we collected the elastic scattering and fluorescence with a parabolic reflector subtending a rather large ($\approx 2\pi$ sr) solid angle. Photomultiplier tube detectors were used to convert the elastic scattering and total (undispersed) fluorescence into electrical signals, which were pulse-height analyzed. Elastic scattering signals were related to particle size with the use of Mie scattering theory. We displayed our results in the form of particle size versus fluorescence histograms,

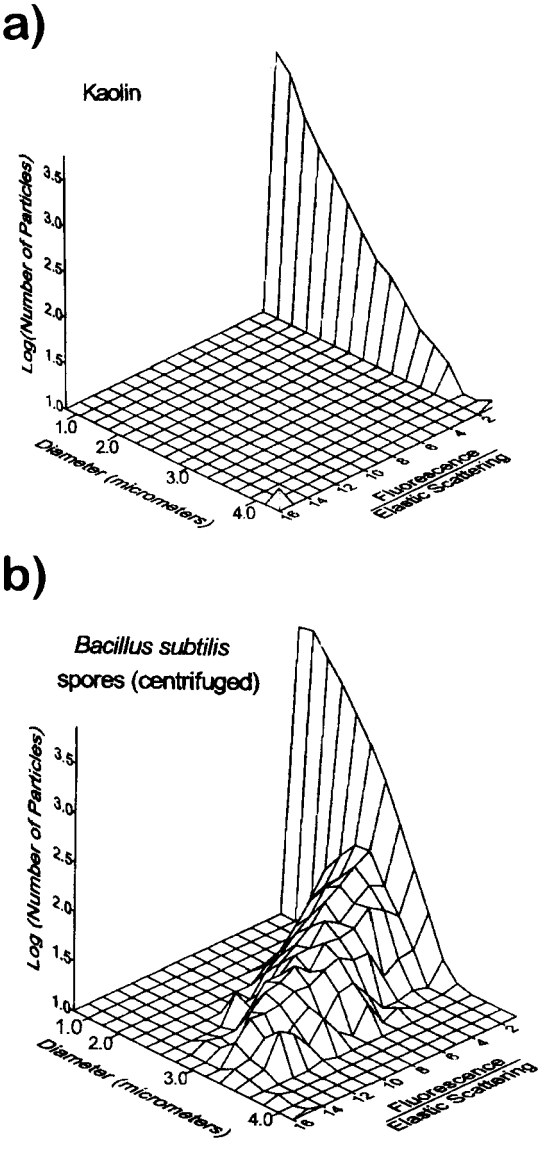

FIG. 1. (a) Histogram of a polydispersion of kaolin particles measured with the fluorescence particle counter (reprinted from Reference 27). The population of particles falls almost exclusively in bins of weak fluorescence. (b) Same as (a), except that the particles are aerosolized *B. subtilis* var. *niger* spores (Dugway Proving Ground, UT), which had been centrifuged to remove some of the soluble materials in the histogram. The large population of weakly fluorescing particles corresponds to dissolved proteins, salts, etc., present in the sample.

as in Figure 1 (from Reference 27). Kaolin [Figure 1(a)] is a common constituent of soil-derived aerosol in arid regions of the earth. *B. subtilis* [Figure 1(b)] is a simulant for *B. anthracis*. The *B. subtilis* particles exhibit far more fluorescence and clearly can be distinguished from kaolin.

Aerosol Fluorescence Spectrum Analyzer (AFSA)

The initial goal of this advance was to upgrade the capability of the FPC to measure single-particle fluorescence spectra.[31] The image of the particle as it traverses the argon-

ion laser beam is imaged onto the spectrograph slit. However, the parabolic reflector in the FPC placed stringent requirements on particle trajectories within the cell, and our attempt to use this reflector was abandoned. We settled for an f/4 lens system that had a significantly smaller collection solid angle (about 0.008 times the 2π sr of the parabolic mirror), with the attendant loss of sensitivity, to collect and focus the light. Because of this small solid angle, and because the CCD detector array could not be gated on for less than a few milliseconds, we were not able to record single-particle spectra. However, we did obtain spectra integrated over ensembles of many particles excited at 488 nm[31] and at 363 nm.[34] The spectra obtained were different for the various biological samples and suggested that spectra may be a useful diagnostic tool for classification. It was clear that this technique would be particularly useful if single-particle spectra could be measured, so that a minority species could be detected, and not be masked by a larger emission coming from the main population of more abundant aerosol particles. Although the 488-nm light does not excite fluorescence of proteins or NADH (a disadvantage for looking at bioaerosols), it also does not excite fluorescence of a variety of nonbiological materials (e.g., napthalene, benzopyrene, various minerals), which are excited at the wavelengths required for excitation of amino acids and NADH. Therefore, there are fewer potential interferents with 488-nm excitation.

Conditional Sampling Aerosol Fluorescence Spectrum Analyzer

To upgrade the capability of the AFSA to measure single-particle fluorescence spectra, we developed a conditional sampling strategy[32] in which an intensified and gateable image-intensified CCD (ICCD) camera is used to record spectra only when a particle of interest traverses the laser beam. Again, the image of the particle trajectory as it traverses the argon-ion laser is imaged along the spectrograph slit. One end of an optical fiber is placed immediately behind a slit aperture at the top of the laser beam at a point where the trajectory of the particle is imaged when it first moves into the laser beam. This fiber is connected to PMT detectors that sense both elastic and fluorescence light scattered by the particle. Signals from these two PMT detectors trigger an ICCD camera, placed at the exit port of the spectrograph, for measuring fluorescence spectra. The image intensifier immediately in front of the CCD detector is triggered only when a particle's trajectory is imaged onto the slit aperture, and is gated to be on only during the time required for the particle to traverse the beam. This arrangement permits the measurement of fluorescence spectra of preselected single particles; that is, particles that exceed a certain size or have fluorescence exceeding a certain threshold voltage on the two PMTs. Other particles are ignored. The system was shown to be able to record the fluorescence spectra of a few interesting particles mixed in a cloud of background aerosol.

Conditional Firing AFSA with UV Excitation

A limitation of the previous work is that the argon-ion laser used (with output at 363 nm and longer wavelengths) is unable to excite the fluorescence of the aromatic amino acids, and at the stronger lines (e.g., 488 nm) is also unable to excite fluorescence of NADH and related compounds, some of the primary fluorophors in biological materials. In order to excite fluorescence of amino acids found in bioaerosol particles, UV excitation at wavelengths below about 300 nm are required (these wavelengths also excite NADH compounds, which can absorb at wavelengths as large as about 380 nm). CW UV energy below 300 nm is available from argon-ion lasers, but the efficiency and output energy is low enough that these lasers are not ideal for obtaining spectra of rapidly moving particles (slowing the particles below a few meters/second would allow better spectra to be obtained, but at the cost of a decrease in sample rate). Thus we decided to exploit the availability of pulsed, triggerable, UV lasers to improve the capability of our detector. In this advance[33] particles being sampled first traverse a visible cw laser beam, where their undispersed fluorescence and elastic scattering are measured with photomultipliers. When the photomultiplier output levels meet preset logic conditions, a UV probe laser (at 266 nm) is triggered to fire and illuminate the targeted particle that had just traversed the visible cw beam. The resulting UV-excited fluorescence spectra are measured with an ICCD camera (placed at the exit port of a spectrograph) which is triggered to be on when the pulsed laser fires. This system can measure the fluorescence spectra of single micrometer-sized biological particles. However, the SNR is only moderate[34] because the solid angle subtended by the collection optics is relatively small,[54] (because of the relatively poor spatial quality of the UV laser[55] and the chromatic aberration in the UV collection optics).

Conditional Firing AFSA with UV Excitation, Cross-Beam Triggering, and Reflective Optics

In order to increase the SNR of single-particle fluorescence spectra, we made three key improvements in our detection system:

1. To more efficiently excite fluorescence in microparticles, we use a more tightly focused pulsed UV probe laser with superior spatial beam quality and a longer pulse length, which is easily triggerable on demand. The higher-quality spatial profile allows for higher intensity at the focal point and more uniformity in measured spectra of particles traversing different parts of the beam, and the longer pulse length provides for multiple excitation of fluorescent molecules during a single pulse (the lifetime of tryptophan is $\approx$3 ns, and the newer pulse lengths are $\approx$27 ns and $\approx$120 ns).
2. To increase our fluorescence signal, we employ a large numerical aperture reflecting objective that can collect fluorescence from the emitting particle over a significantly larger solid angle, and still focus it onto the slit of a spectrograph without chromatic aberration.

3. In order to define a small sample volume through which particles must move in order to be sampled (required because the tightly focused probe laser must overlap with the focal region of the large numerical aperture collection objective), we require the particles to pass through two crossed cw-diode laser beams that are focused immediately upstream from the UV probe laser.

Figure 2 illustrates schematically our experimental setup, which is not yet in a field-portable configuration. Particles entrained within a stream of air emanating from an ink-jet aerosol generator[56] (used here for generation of test aerosol) are directed downward toward the sample volume. As noted previously, we met the requirement for a precisely defined sample volume by using two nearly orthogonal diode-laser beams having different wavelengths (635- and 670-nm) which precisely define an $\approx$20-μm-diameter focal volume centered in the focal region of the UV laser beam, and in the focal plane of the reflecting objective. Particles must pass through the intersection of both of these focused-trigger beams before a logic pulse triggers the UV laser to fire and the intensifier of the ICCD to turn on. Thus, particles not flowing through this region, which are not illuminated by the central portion of the UV laser beam and not in the focal region of the Schwarzschild objective, are ignored.

Details of this sampling strategy are as follows. Figure 2 shows an aerosol particle flowing through the focal volume of the crossed beams. The near-forward elastic scattering is measured with two photomultipliers (PMT 1 and PMT 2, with narrow-band interference filters at 670 nm for diode-trigger laser 1 and 635 nm for diode-trigger laser 2). The two PMT signals are fed into two single-channel analyzers (SCA 1 and SCA 2) set to operate as discriminators in a window mode. The PMT pulses must exceed the preset lower voltage level (set in the threshold mode) before the SCA provides an output pulse. The two SCA outputs are fed into a logical AND gate, which produces an output pulse only when the SCAs send out signals that overlap in time. The AND gate output then sends a trigger pulse to the Q-switched laser[57] and to the controller of the ICCD.[58]

The system can also be operated in a conditional firing mode in which fluorescence spectra are measured only for particles falling within a preset size interval. In this mode, another restriction is placed on particles before the UV probe laser is triggered to fire and the ICCD intensifier is gated on. In addition to requiring that particles pass through both diode laser beams, we require that they have sizes within a certain interval. We accomplish this by requiring that the intensities of the diode-laser light scattered by the particle fall within preset intervals; that is, the SCAs are set in the window mode.

Samples and Aerosol Generation

Biological Samples

Several of the samples were used as purchased: meadow oat pollen allergens (Greer Laboratory), paper mulberry pollen (Duke Scientific), *B. subtilis* [vegetative cells, American Tissue Culture Collection (ATCC) 6633, Sigma Chem.], *B. subtilis* var. *niger* spores (Dugway Proving Grounds, UT), *Erwinia herbicola* (ATCC 33243), fungal spores (*Aspergillus versicolor*, ATCC 9577). *B. subtilis* var. *niger* (vegetative cells), and *E. herbicola* were also grown by streaking onto tryptic soy agar plates.

Chicken-house samples were collected from a poultry house with the use of a one-stage cyclone. The cyclone was operated to have a 50% cutoff of 0.8–1.2-μm aerodynamic diameter. The dust was removed from the collection surface and stored in a refrigerator prior to re-aerosolization.

Other Samples

Arizona road dust samples were obtained from Powder Technology Corporation, Burnsville, MN; ammonium sulfate and ammonium nitrate samples were from Sigma Chemical; carbon black was obtained from Cabot Corporation.

Aerosol Generation

An Ink Jet Aerosol Generator[56] (IJAG), (see right inset in Figure 2) was used to generate test aerosols. The IJAG produces dry aerosol particles that are somewhat monodispersed (typical standard deviation in size distribution is $\approx$15%). The material to be aerosolized in the IJAG is suspended in distilled, deionized, filtered water and then inserted into an ink-jet cartridge (HP 51612A, purchased empty) having 12 nozzles. Each cartridge nozzle is activated through its resistive heater to generate a droplet approximately 50 μm in diameter, plus one or two smaller satellite droplets. Droplets are generated sequentially in the 12 nozzles at a frequency we selected to be between 1 Hz and 2 kHz, or singly on demand. These droplets are ejected downward, carried by a filtered stream of air, and passed through a drying chamber heated to about 104° C. As the droplets traverse the drying chamber, their water evaporates, leaving the residual particles. Smaller aggregates produced from the satellite droplets are swept out of the drying chamber with the use of a purge flow system. Because the size of the primary ink-jet droplet is fixed, the size of the dried particle depends only on the initial sample concentration in the water suspension. For this series of measurements we have in most cases prepared 0.1% suspensions by weight, resulting in 5-μm-diameter dried particles. A dedicated controller operates the ink-jet cartridge and drying chamber. At the exit port of the generator, the dried particles are carried in an air stream through a tapered 1-mm-diameter exit nozzle.

An Aerodynamic Particle Sizer, model 3310A (Thermal Systems, Inc., Minneapolis, MN) was used to obtain an aerodynamic-size distribution of the particles in real time. In most cases, the aggregate sizes were also measured with the use of scanning electronic microscope (SEM) images of particles collected onto filters.

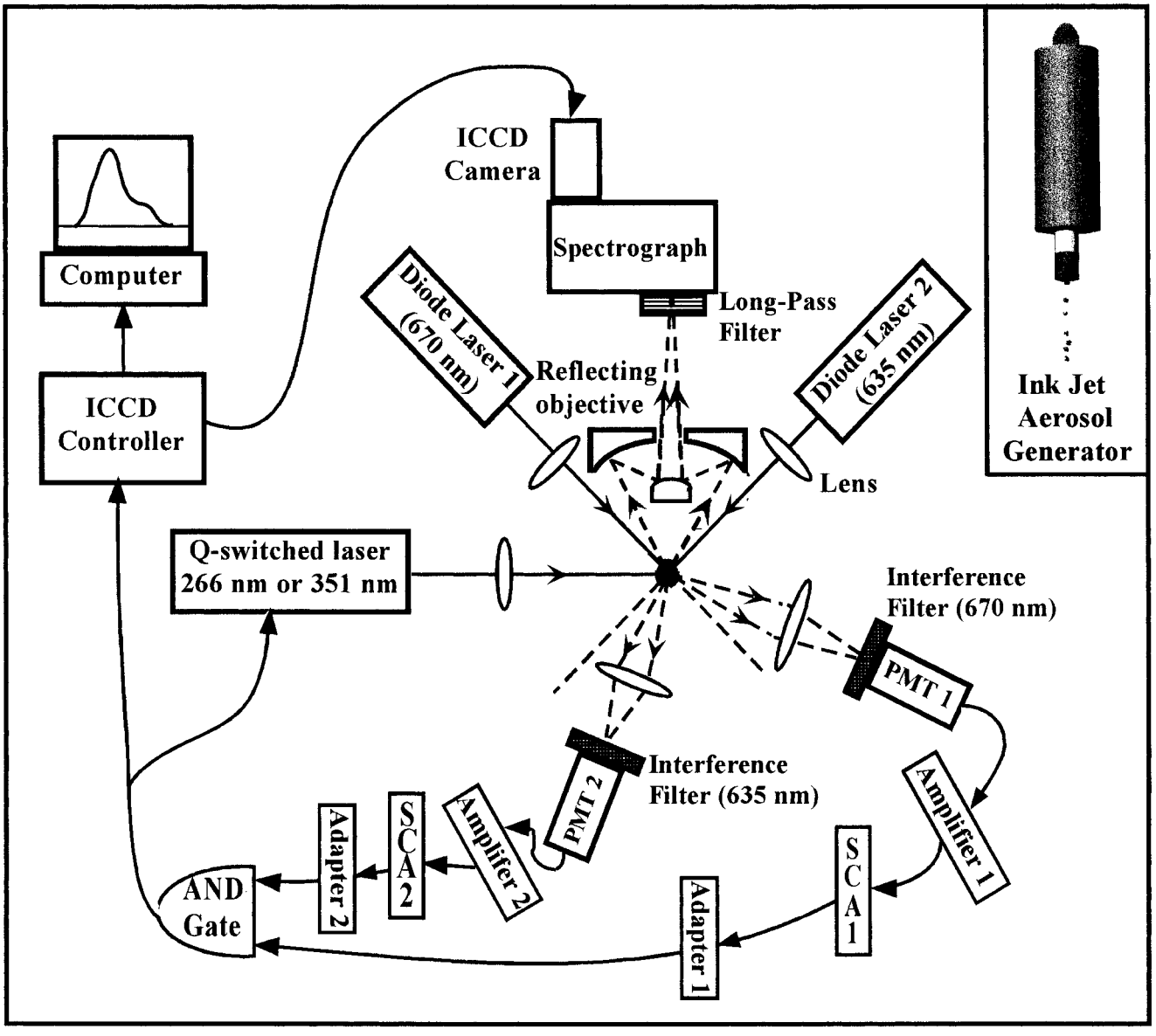

FIG. 2. Schematic of the AFSA setup used for detecting single-shot laser-induced fluorescence spectra from individual micrometer-sized aerosol particles. The sample volume is defined by two intersecting continuous-wave diode laser beams (at 635 and 670 nm). When a particle traverses the sample volume: (1) it scatters the light from the two diode-laser beams; (2) this near-forward scattered light is detected by photomultipliers PMT1 and PMT2; (3) if the signals from both PMTs fall within preset voltage windows, each single-channel analyzer (SCA) produces an output; (4) if each of SCA's outputs are logical ones, the AND gate indicates that a spectrum is to be measured for this particle (by sending a triggering signal to the UV laser and the intensified CCD detector); (5) the Q-switched UV laser fires and excites fluorescence in the particle; (6) the fluorescence is collected by the reflecting objective and focused onto the input slit of the spectrograph; (7) the spectrograph disperses the emission energy; and (8) the fluorescence spectrum is recorded with the intensified CCD, which is gated to be on when the UV laser fires. The inset is a representation of the ink-jet aerosol generator (IJAG) used for generation of test particles.

Results and Discussion

Spectra of Fluorophors Found in Biological Particles

To initially test the AFSA we measured the spectra of some of the primary fluorophors in biological aerosols (tyrosine, tryptophan, NADH, and riboflavin). Spectra for these compounds in solution are well known.[49,50] We dissolved these materials in water and aerosolized the solutions with an IJAG. Spectra for single (nominal 5-μm-diameter) particles of these fluorophors are presented in Figure 3. With 266-nm excitation, the amino acids tyrosine and tryptophan have peak emission around 310 nm and 340 nm, respec-

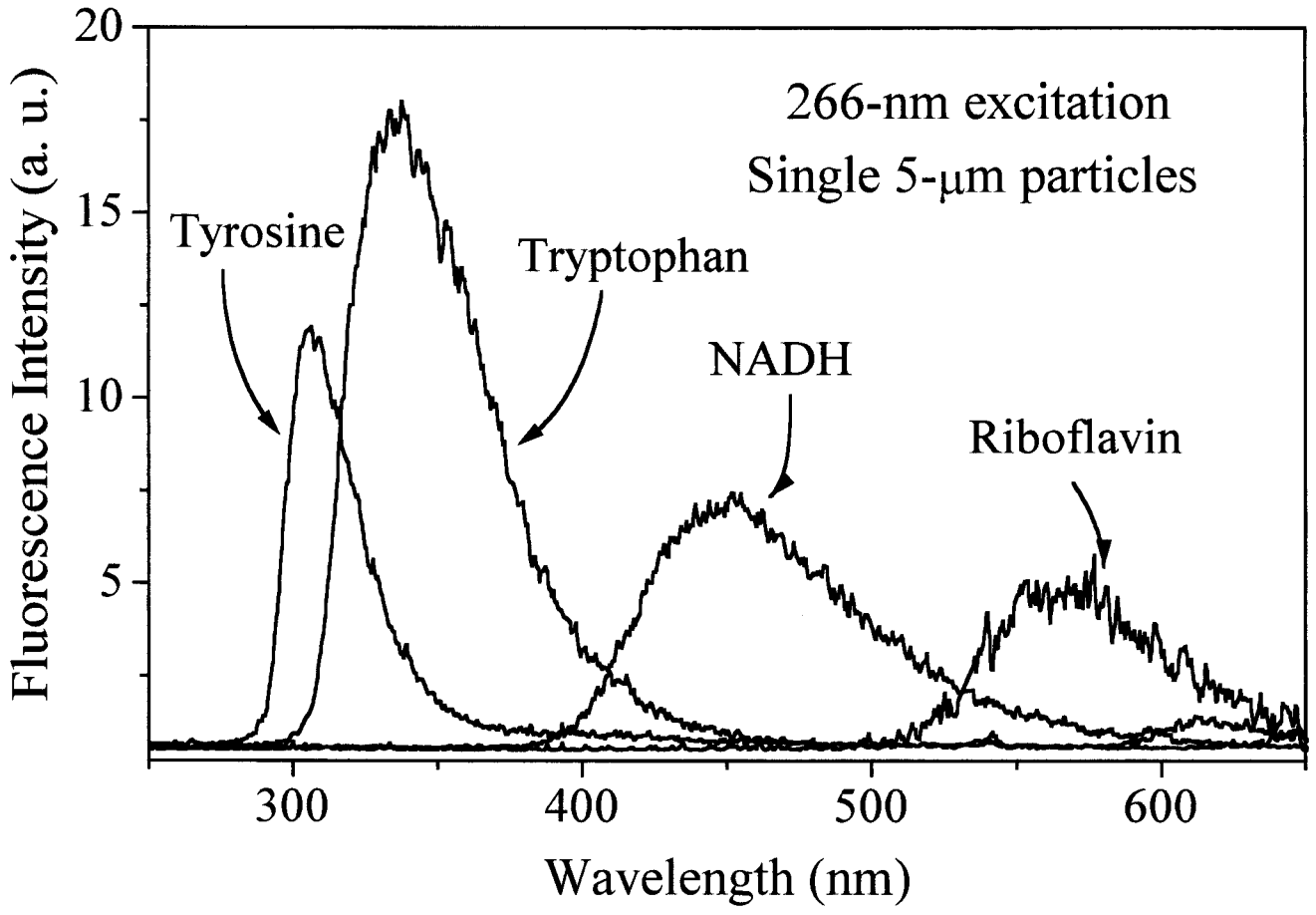

FIG. 3. Single-particle 266-nm-excited fluorescence spectra of common fluorophors found in biological particles. Each spectrum is for a nominal 5-μm-diameter particle measured with the AFSA. The tyrosine intensities below 300 nm appear to be reduced by the absorbance of the filter (N,N-dimethylformamide) used to block the 266 nm scattered light.

tively, the NADH emission peaks around 450 nm, and riboflavin emission from dry particles peaks near 560 nm. Because these peaks occur in different spectral regions, we expect that some simple classification of biological particles may be possible from their fluorescence spectral signatures.

Repeatability of Fluorescence Spectra of Uniform Particles

We show the sensitivity and reliability of the AFSA detection system with *E. coli*. The overall fluorescence quantum efficiency of dry *E. coli* excited with 266-nm light may be about 3% of that of pure tryptophan (based on the fraction of the dry weight of *E. coli* that is tryptophan). The uniformity of the fluorescence spectra from single nominal 4-μm-diameter particles of dried *E. coli* is exhibited in the sequence of 10 consecutive spectra in Figure 4. The broad fluorescence peak at 350 nm is mainly from tryptophan, and the tail from 400 to 500 nm is attributed to fluorescence from residues of the nutrient growth material (which may have contributions from reduced nicotinamide compounds). The sharp peaks at 266, 532, 635, and 670 nm are from leakage of the 266-nm beam, the 532-nm beam that generates the 266-nm light, and the two cw diode lasers, respectively. (In these spectra the peaks at 266 and 532 nm are larger than in some of the subsequent figures, probably because in this figure something nearby scattered more light toward the lens—the background is sensitive to the alignment and to the positions of beam blocks.) The 635- and 670-nm peaks have been truncated for clarity of presentation. The spectra shown in this figure are similar from particle to particle and demonstrate that the system can capture, in real time, the fluorescence spectra of fairly low quantum-efficiency, micrometer-sized bioaerosols with a high SNR and good spectral resolution.

Detection of Rare Bioaerosol Particles Mixed in Background

Unlike the uniform *E. coli* bacteria shown previously, the biological particles of interest for field applications may be entrained with other aerosol particles that comprise the background. Average fluorescence spectra (which are the sum of

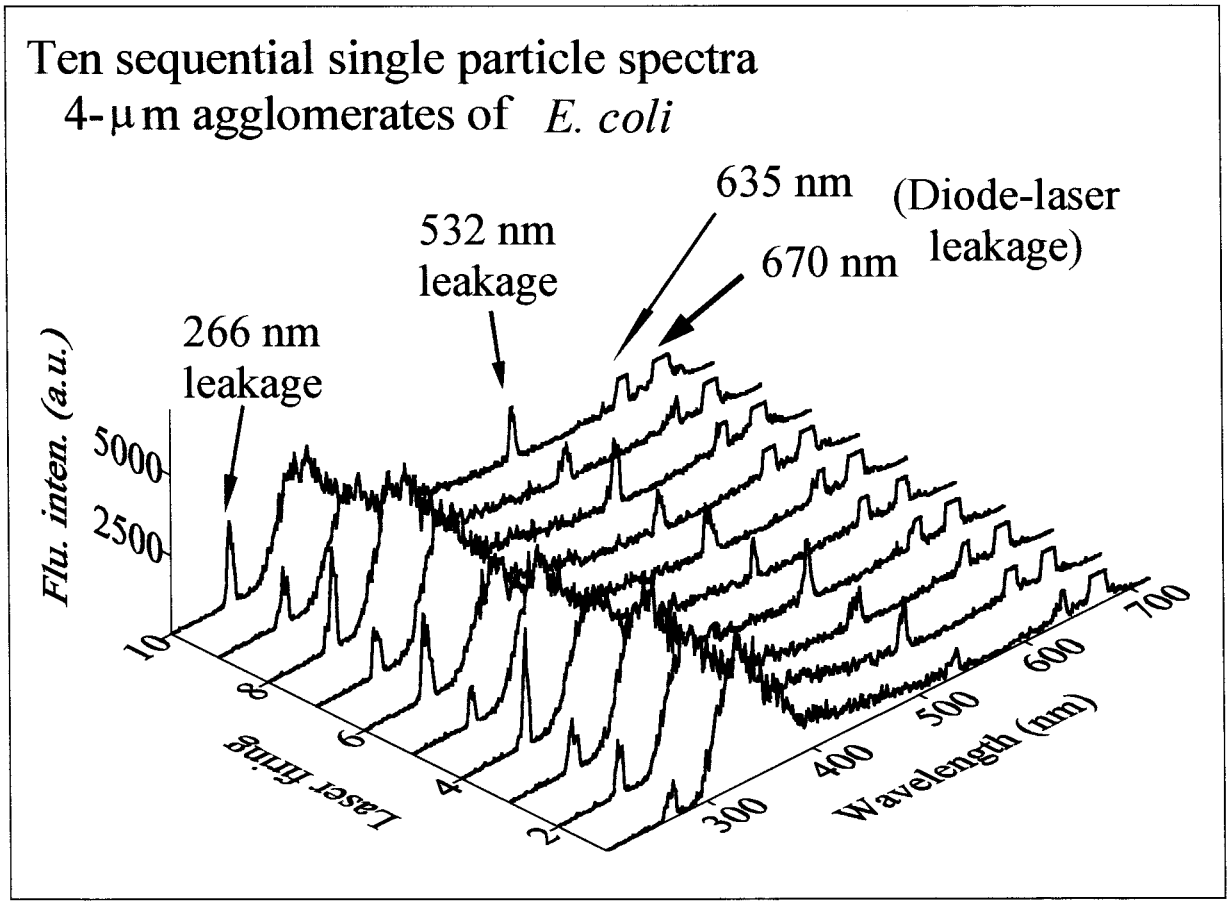

FIG. 4. Ten consecutive single-particle fluorescence spectra of nominal 4-μm-diameter particles composed of *E. coli* bacteria. The spectra-to-spectra variations are relatively small, demonstrating that the AFSA can measure the fluorescence spectra of nearly uniform particles repeatedly, with a good SNR. Leakage from the exciting 266-nm laser, the 532-nm laser generating the 266-nm beam, and the diode trigger lasers is evident in each spectrum.

the spectra for many aerosol particles) may yield little or no information about the few particles of interest. Hence, it is important for a field-portable detector to be able to measure good-quality spectra from single particles as they are sampled from a complex mixture.

This capability of our detection method is demonstrated in Figure 5, which shows 20 consecutive single-shot fluorescence spectra of particles generated from a sample collected from a chicken house. The sample was mixed with water and aerosolized with the use of the IJAG. The average particle diameter was approximately 3 μm. Most of the fluorescence spectra are similar to the single-shot spectra labeled (a) in the inset (these have a broad emission from about 300 to 600 nm). The more smooth line in (a) overlapping the single-shot result shows the average spectrum of the 100 consecutive single shots. The spectra labeled (b) and (c) in the inset show the 4th and 48th fluorescence spectra from the series of 100 single shots. These are distinctly different from the other spectra. The 4th spectrum [curve (c)] has a band with two peaks located near 320 nm and a broader band that peaks around 450 nm. The 48th spectrum [curve (b)] has its strongest emission closer to 350 nm.

Chicken-house dusts are complicated, with a large variety of microbes mixed in a background of organic, inorganic, and biological matter. In the sample measured here the total culturable microbial component is only 1% of the weight, and the culturable fungal species make up less than 0.006% of the weight.[59] The dominant bacterial species are *Staphylococcus aureus* and *Brevibacterium* sp. The uniformity of the large majority of the spectra in Figure 5 suggests that the major fluorescing component of these particles is either soluble or is in the form of very small particulates so that the fluorophors are distributed somewhat uniformly in the suspension used in the IJAG. The fact that the 4th and 48th spectra exhibit much larger and spectrally distinct fluorescence suggests that some of the fluorescing material is not uniformly dispersed in the suspension. Our detection method is able to differentiate these uncommon particles from the background. This figure demonstrates the capability of the AFSA to detect rare particles that are mixed with a dominant concentration of background particles.

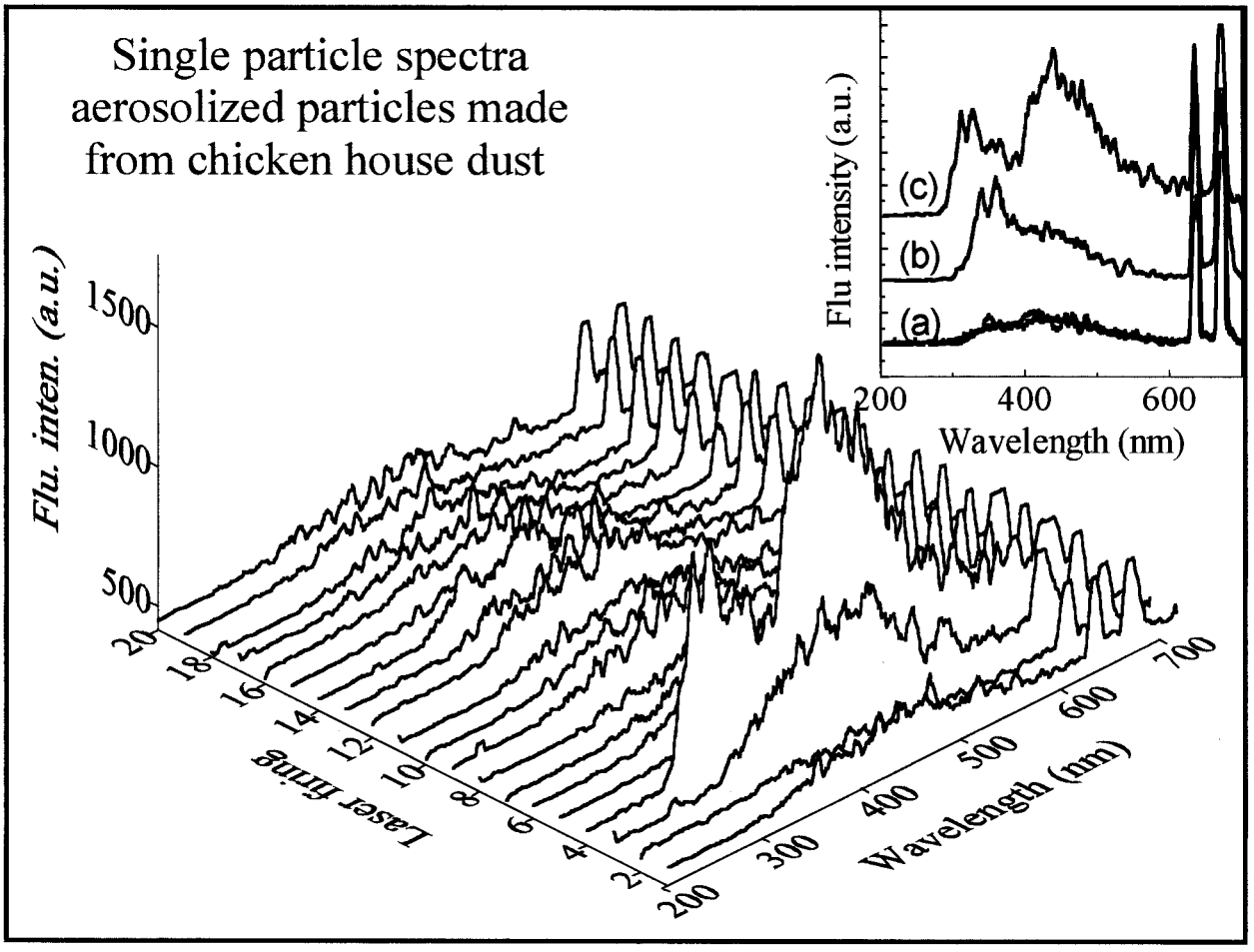

FIG. 5. Twenty consecutive single-particle 266-nm-excited fluorescence spectra of aerosolized particles (nominal average diameter is 3 μm) generated from chicken-house dust (the dust was mixed with water and aerosolized with the ink-jet generator). The variability in the spectra indicates differences in particle-to-particle composition. Three single-particle spectra for the 2nd, 4th, and 48th laser shots are shown in the inset. Most spectra are similar to the single-shot spectra labeled (a) in the inset, which is in good agreement with the 100-particle average [smoother line in (a)]. The spectra labeled (b) and (c) in the inset are for the minority of particles in the sample that have distinctly different fluorescence signatures than those of the main population of particles.

Differentiation of Biological and Nonbiological Aerosols Using Fluorescence Spectra

In many environments the dominant background particles are nonbiological (a minority concentration of bioaerosols must be differentiated from these nonbiological particles).

Spectra for aerosols composed of some common nonbiological atmospheric aerosol constituents (ammonium sulfate, soil-derived dust consisting of quartz and clay minerals, black carbon, and ammonium nitrate) are compared to the spectra of a bacterial spore, *B. subtilis* var. *niger* (Dugway) in Figure 6. As before, we mixed these materials in water (either in solution or suspension), and aerosolized the mixture with an IJAG to create nominal 5-μm-diameter particles. Each spectrum is an accumulation of 100 particles (summing the spectra to increase the SNR is necessary for the weakly fluorescing nonbiological samples). Compared to *B. subtilis*, nonbiological particles contribute little fluorescence in the 300- to 350-nm region, and their fluorescence at longer wavelengths is also weak. The results suggest that, for equal mass particles, the total undispersed fluorescence intensity may be sufficient to separate biological particles from at least some common nonbiological particles. The results also suggest that spectral differences could also be useful in distinguishing between biological and nonbiological particles, regardless of their size.

Distinguishing Bacteria from Other Biological Particles

In addition to discriminating between biological and nonbiological particles, we want to distinguish bacterial aerosol from other biological particles. In Figure 7 we present fluorescence spectra of a bacteria (*B. subtilis* var. *niger*, vegetative cells) compared to meadow oat pollen, tobacco leaves, and cigarette ash. All spectra are for single nominal 5-μm-diameter particles. Clearly the bacteria can be differentiated from some common biological particles that are not bacterial. Additional examples were shown previously.[35]

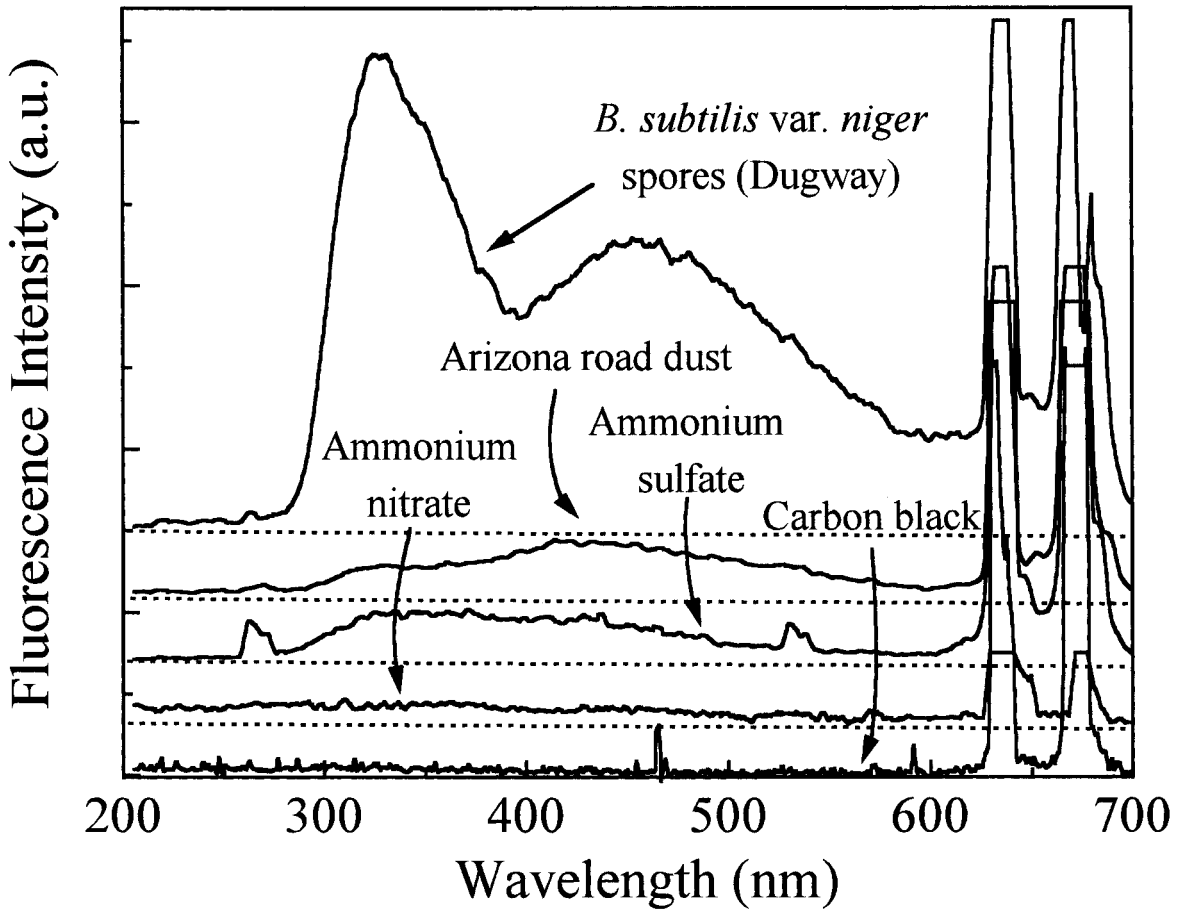

FIG. 6. Fluorescence spectra, excited at 266 nm, of a bacterium and common atmospheric particles (from top to bottom) *B. subtilis* var. *niger* (spores, Dugway), soil-derived dust consisting of quartz and clay minerals (Arizona road dust), ammonium sulfate, ammonium nitrate, and black carbon. These materials were mixed in water (solution or suspension) and aerosolized with an IJAG. Each spectrum represents an accumulation for 100 nominal 5-μm-diameter particles.

Inability to Distinguish Different Washed Bacterial Aerosols

Previous measurements of aerosolized bacteria suggest that well-washed bacteria have similar fluorescence spectra.[37,53] Fluorescence spectra (with the use of 266-nm illumination) accumulated for 100 nominal 5-μm-diameter particles of washed bacteria (*B. subtilis*, *E. herbicola*, and *E. coli*) are presented in Figure 8. The spectra are normalized at the strong fluorescence peak around 330 nm. The comparison reveals that all spectra are similar with a strong fluorescence peak around 330 nm originating from the contribution of tryptophan, and shoulders in the 400- to 500-nm regime. Small differences in the accumulated spectra are not evident for single particles because the SNR is poorer for single-shot measurements. Thus, at least for these samples, our technique is not able to distinguish different species of washed bacteria, in agreement with previous findings.[37,53]

Distinguishing the Same Bacteria Prepared Differently

If our detection system cannot differentiate among bacteria, can it discriminate between the same bacteria prepared differently? Spectra for nominal 5-μm-diameter *B. subtilis* vegetative cells (Sigma), *B. subtilis* var. *niger* spores (Dugway), and washed and unwashed *B. subtilis* var. *niger* vegetative cells are presented in Figure 9. The spectra are normalized to the 330-nm tryptophan peak, and show different spectral features in the 400–500-nm spectral region. Clearly, some preparations of the same bacteria can be distinguished by their spectra.

Distinguishing Washed and Unwashed Bacteria

Figure 10 presents the fluorescence spectra accumulated for 100 nominal 5-μm-diameter particles of washed and unwashed *E. herbicola* obtained with 266-nm excitation; also shown are spectra for similar-sized particles of the supernatant. Spectra for unwashed *E. herbicola* show a fluorescence peak around 330 nm, mainly from tryptophan, and a weaker peak near 440 nm, which probably has contributions from nutrient growth material and possibly reduced nicotinamide compounds. In the washed sample the 330-nm tryptophan peak is reduced in amplitude and the smaller 440-nm peak nearly disappears. The curve that is the sum of the

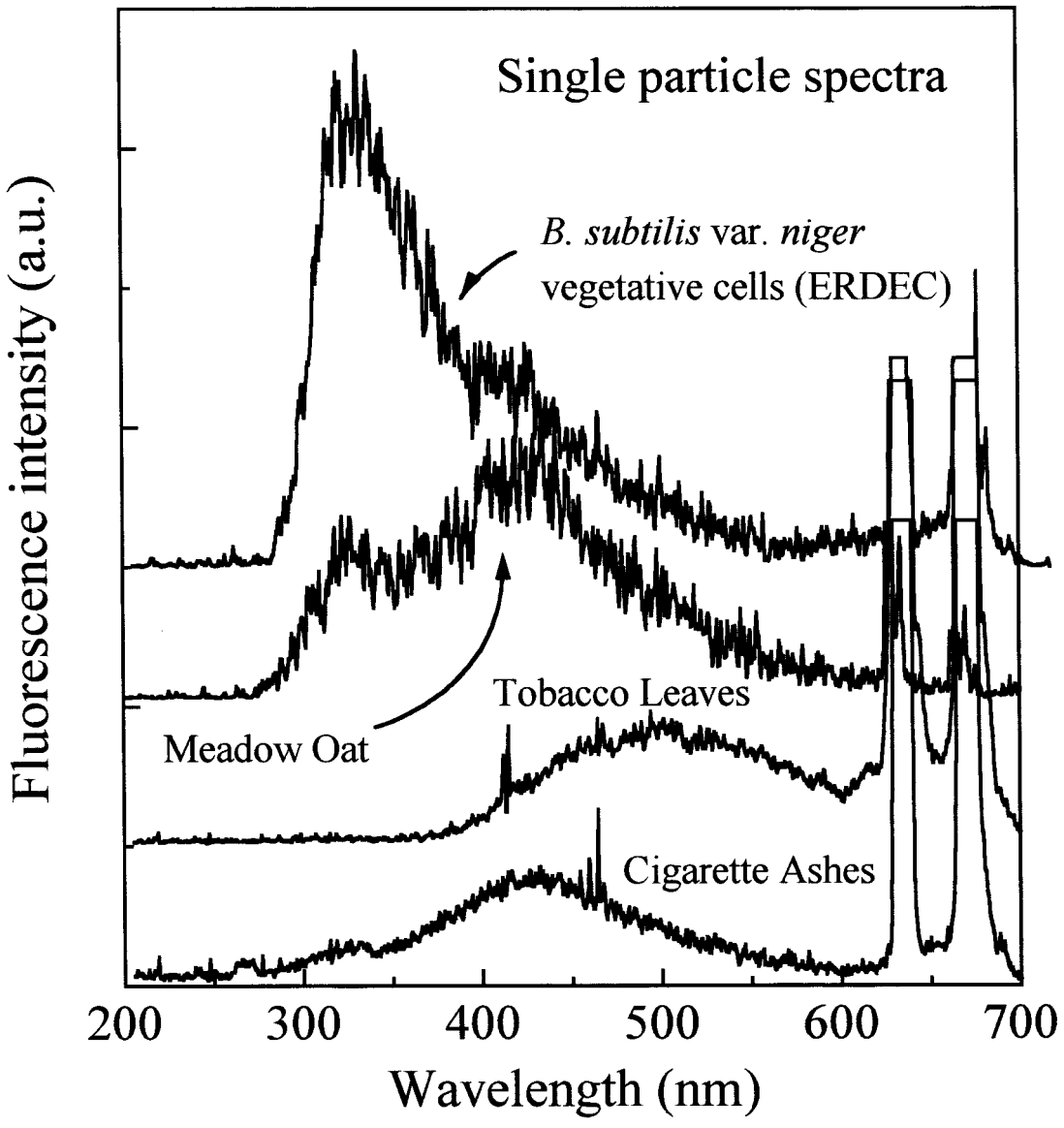

FIG. 7. Single-particle fluorescence spectra (excited at 266 nm) of nominal 5-μm-diameter particles of *B. subtilis*, var. *niger*, meadow oat pollen, tobacco leaves, and cigarette ash. The spectra are distinctly different, demonstrating the capability of the AFSA to distinguish a bacterial particle from common nonbacterial, biological particles.

fluorescence from the washed *E. herbicola* and its supernatant matches closely the spectra of the unwashed sample, suggesting that the 440-nm peak is attributable to water-soluble compounds.

Advantage of Multiple-Wavelength Excitation for Bioaerosol Discrimination

Some bioaerosols excited at 266 nm have nearly the same fluorescence spectral signature. The example in Figure 11(a) shows fluorescence spectra of fungal spores and *B. subtilis* var. *niger* vegetative cells, both 5 μm in diameter. The spectra are dominated by tryptophan and are similar for the two samples. On the other hand, the spectra of the same samples excited at 351 nm [see Figure 11(b)] are different. Because the 351-nm photon energy is too low to excite fluorescence from amino acids, their fluorescence is not observed and consequently the fluorescence is dominated by other compounds (possibly flavins, NADH compounds, or growth materials).

The inability to differentiate bioaerosols with the use of spectra can also occur with 351-nm excitation. Figure 12 shows fluorescence spectra of washed and unwashed *B. subtilis* var. *niger* vegetative cells excited by 266- and 351-nm light. The spectra are nearly indistinguishable with 351-nm excitation, yet are different with 266-nm excitation.

The conclusion that can be drawn from this comparison with two judiciously chosen excitation wavelengths is that multiwavelength excitation of fluorescence spectra can sometimes distinguish between samples that cannot be dis-

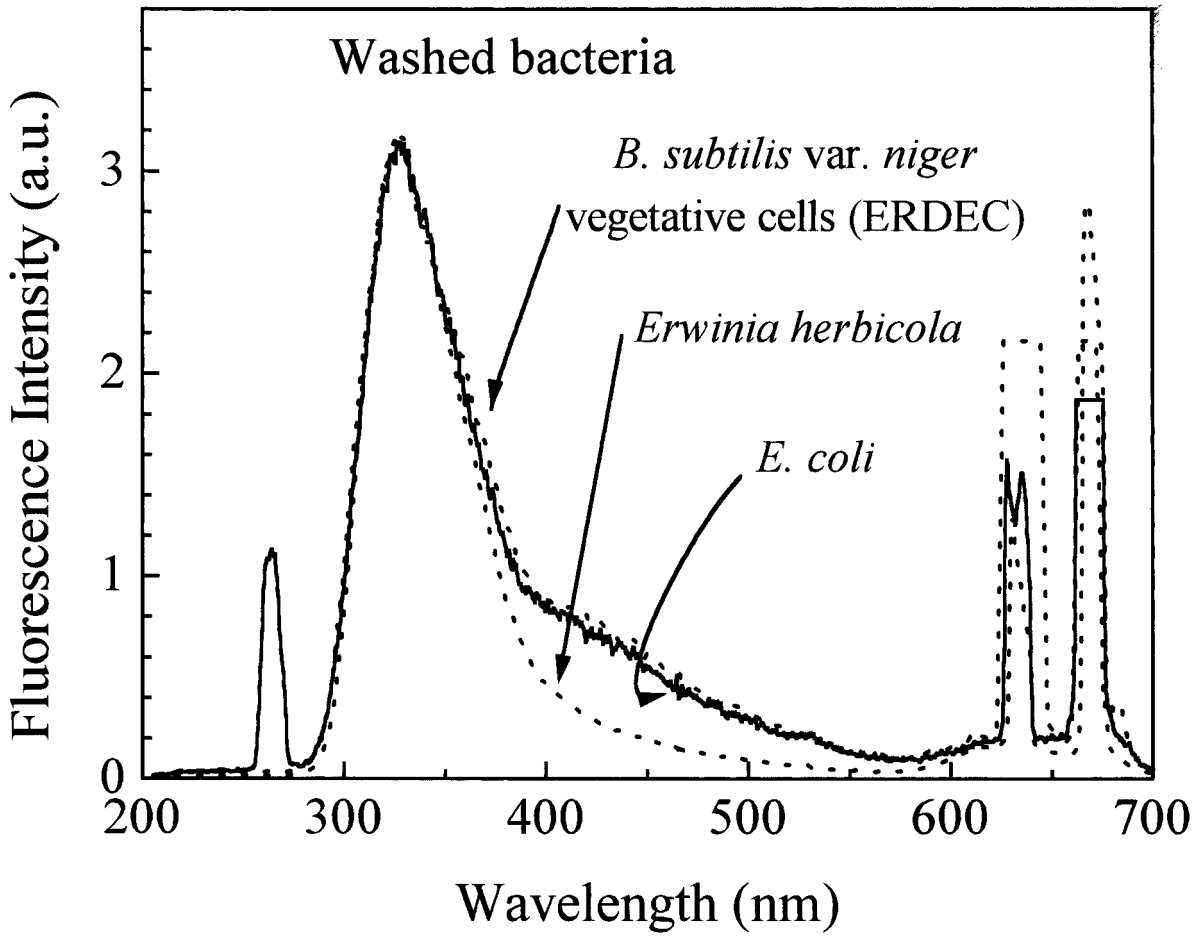

FIG. 8. Fluorescence spectra (excited at 266 nm) of washed bacteria: *B. subtilis*, *Erwinia herbicola*, and *E. coli*. All spectra are averages for 100 nominal 5-μm-diameter particles and have been normalized to the peak fluorescence at 330 nm. The spectra are nearly the same, revealing the inability of the AFSA to differentiate among washed bacteria.

tinguished with the use of only a single-excitation wavelength.

Tobacco Smoke and B. subtilis *Have Similar Fluorescence Spectra*

Environmental tobacco smoke is a common bioaerosol that might interfere with attempts to detect bacteria. It is also an important pollutant; its monitoring may be an application of an AFSA. We term it a bioaerosol even though it includes burned and partially burned materials.

Figure 13 shows the 266-nm-excited fluorescence spectra of sidestream cigarette smoke and *B. subtilis* var. *niger* vegetative cells (averages of over 100 single shots in each case). The spectra are normalized to have similar heights. A lighted cigarette was held within a few centimeters of the apparatus and the sidestream smoke drifted into the sample region.

The thresholds for the PMT voltages were set high enough that individual tobacco particles (which are predominantly submicron in size[60]) did not trigger the laser. Because sidestream tobacco smoke consists of a high concentration[61] of submicron particles, there were likely multiple particles in the sample volume (perhaps as many as 100). Thus, the spectra shown are probably from multiple smoke particles that were in the sample region. The relatively poor SNRs of the single-shot tobacco-smoke spectra (not shown) are consistent with the total volume of the smoke particles being smaller than the volume of the single *B. subtilis* aggregates (nominal 5-μm-diameters). In addition, the smoke may have different fluorescence per unit volume.

Interestingly, the peak position and line shape of the fluorescence spectra of the tobacco smoke and *B. subtilis* are similar, except that the tobacco smoke has more fluorescence in the 280–310-nm range, and has a small bump between 560 and 610 nm (peaking at about a 30-nm longer wavelength than riboflavin). Because the differences between the spectra are relatively small, and because the single-shot tobacco-smoke spectra have relatively poor SNR, we expect that with the existing setup it may not be possible to distinguish individual micrometer-sized tobacco smoke particles from similarly-sized bacterial particles.

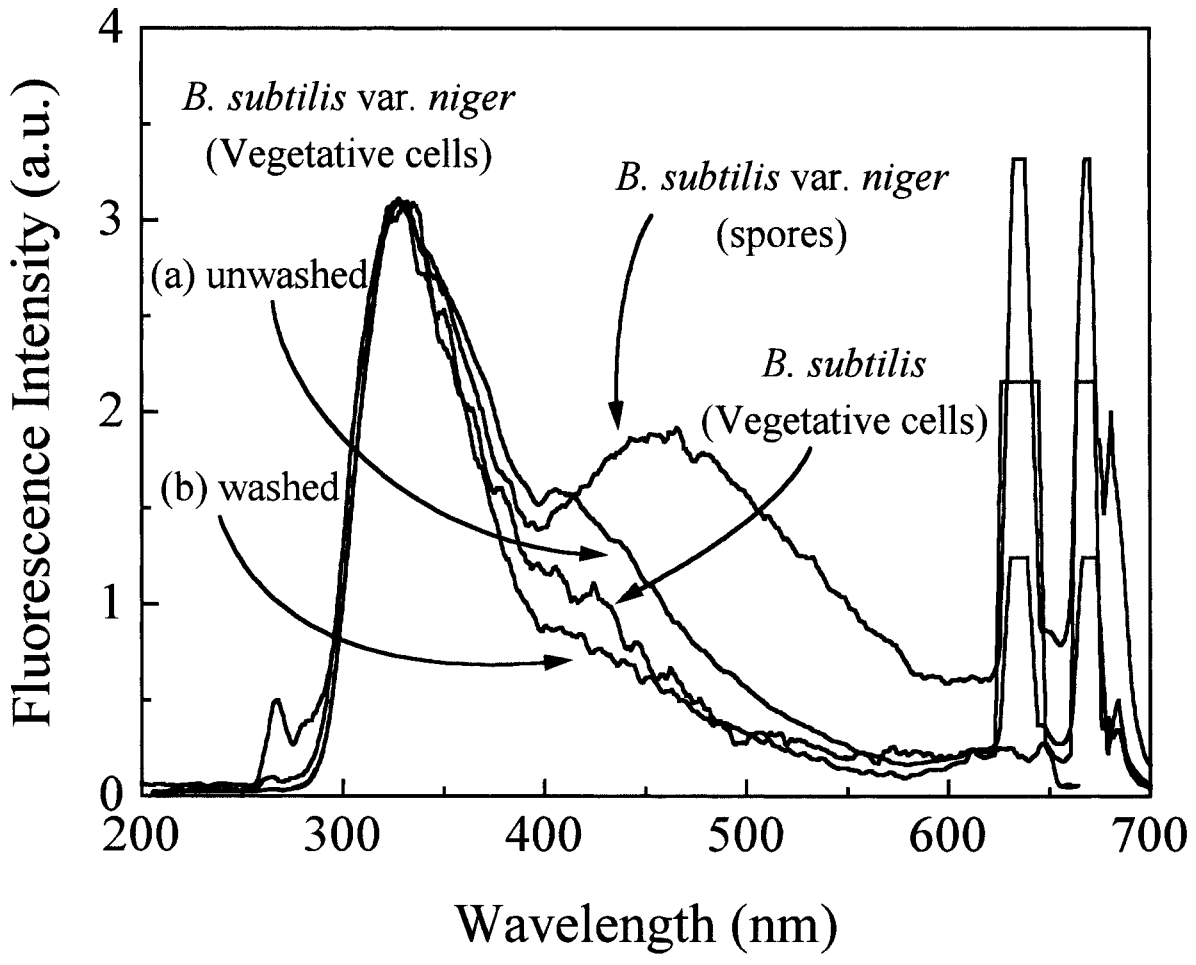

FIG. 9. Fluorescence spectra (excited at 266 nm) of different preparations of *B. subtilis*: washed and unwashed var. *niger* vegetative cells, var. *niger* vegetative spores, and vegetative cells. All spectra are averages for 100 nominal 5-μm-diameter particles. The spectra are distinct, suggesting that the AFSA can distinguish different preparations of the same bacterium.

Discussion

Potential Utility of the AFSA

Determining the potential usefulness of the AFSA for classifying atmospheric bioaerosols will require further investigation. To date, all of our measurements, and those of others,[37,53,62] were taken on laboratory-generated aerosols or samples in suspension. No data on the UV-excited fluorescence spectra of real atmospheric bioaerosols appear to be available.[63] In natural atmospheric environments individual biological aerosol particles will be, in many if not most cases, complex mixtures of biological and nonbiological materials, not simply the relatively pure samples of bacteria or pollen allergens we have studied here. For example, when droplets are generated in wave action of a lake or pond, a droplet that evaporates to form an aerosol particle may contain multiple types of bacteria, dissolved decaying plant material, and inorganic salts that are dissolved in the pond water. Each particle containing the residue of the dried droplets will be a complex mixture. In agricultural or industrial environments, bacteria, fungi, and viruses may agglomerate with other aerosol particles.

We are striving toward developing a capability to measure spectra of natural and anthropogenic bioaerosols in a variety of environments. Our goal is a system that can work in complex atmospheric environments (urban, agricultural, hospital, workplaces, etc.), with the capability of indicating if the aerosol is biological or not, and, if biological, of classifying the bioaerosol into a few (perhaps as many as 30) broad categories based on both spectral features and particle size. (Particle sizes could be determined from elastic scattering signals and would require no additional lasers.)

Field-Portable System

The prospect of transforming the present laboratory AFSA system into a field-portable instrument depends on the size, weight, and power consumption of each of the crucial components. The spectrograph used here could consist of a single, concave, holographically constructed grating.

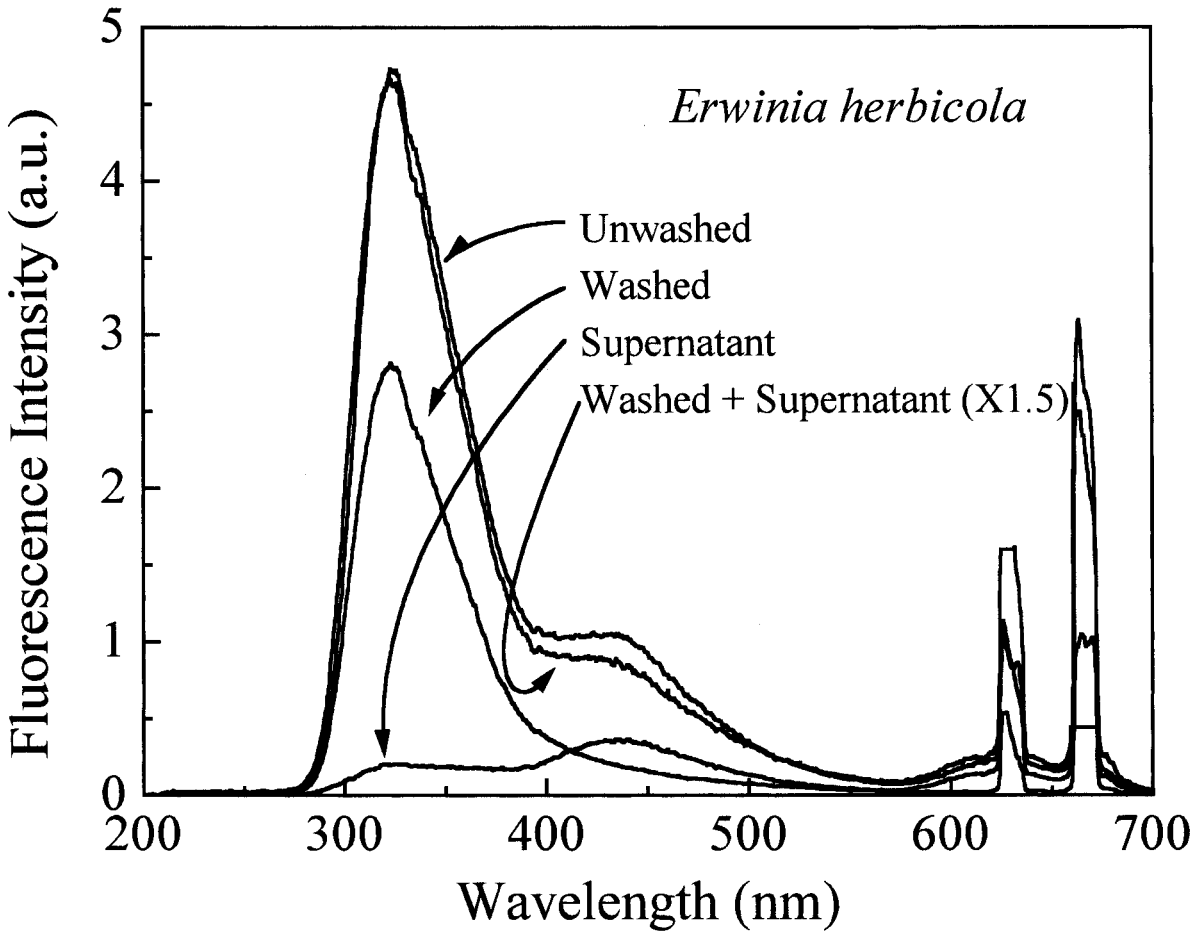

FIG. 10. Fluorescence spectra (excited at 266 nm) of particles of unwashed *E. herbicola*, washed *E. herbicola*, the supernatant, and the washed *E. herbicola* plus supernatant. All spectra are averages for 100 nominal 5-μm-diameter particles. The spectrum for washed *E. herbicola* is missing the 440-nm peak, which appears largely due to soluble nutrient growth material in the supernatant.

The present ICCD detector could be replaced by recently available multianode PMT detectors, which can be powered with small batteries.

Among the components needed for the AFSA, the UV excitation source is the heaviest and consumes the most power. Pulsed UV radiation sources are ideal, because the aromatic amino acids need to be excited in the UV (250–290 nm) range, and the particles transit the focal volume in less than 15 μs. Smaller and more energy-efficient UV sources depend critically on advances in laser and/or nonlinear crystal technology. In the 1970s the meter-long, large-power-consuming, water-cooled, cw, argon-ion lasers (emitting at 351 nm in the UV) were all that were available. In the 1980s flash-lamp–pumped Nd:YAG lasers (1064 nm) that had to be converted to the third and fourth harmonic became available for laboratory use. In the 1990s, with the advancements in GaAs-diode laser-pumped Nd:YAG lasers and nonlinear crystals for more efficient and reliable second, third, and fourth harmonic conversions, pulsed blue (355 nm) and UV (266 nm) sources became accessible. The miniaturized microchip Nd:YAG laser that is self Q-switched, GaAs-diode laser-pumped, and fourth harmonic convertible is an example of how far laser technology has advanced.[30] In the late 1990s, intense research is being conducted in developing blue to near-UV semiconductor lasers. The entertainment industry (with CD and other optical storage technology in particular) is propelling the development of GaN, GaInN, and AlGaN semiconductor diode lasers. Recently, cw blue GaInN lasers (operating over 10,000 h) have been demonstrated.[63] In the next few years the prospects are good for building a field-portable AFSA instrument that contains several pulsed blue- and near-UV-emitting semiconductor diode lasers, reflecting optics, a holographic grating, and a multi-anode photomultiplier.

Sample Rates

The sample rate for the present setup is relatively small. If the sample volume has a 20-μm diameter and the particle flow rate is 10 m/s, the sample rate is $\pi(0.001\text{ cm})^2(1000\text{ cm/s}) = \pi \times 10^{-3}$ cm^3/s. If the particles are concentrated a factor of 300:1 before being introduced to the sample region, then the sample rate increases to 1 cm^3/s, or only 0.06 l/min. (The sample rate is necessarily small because the interro-

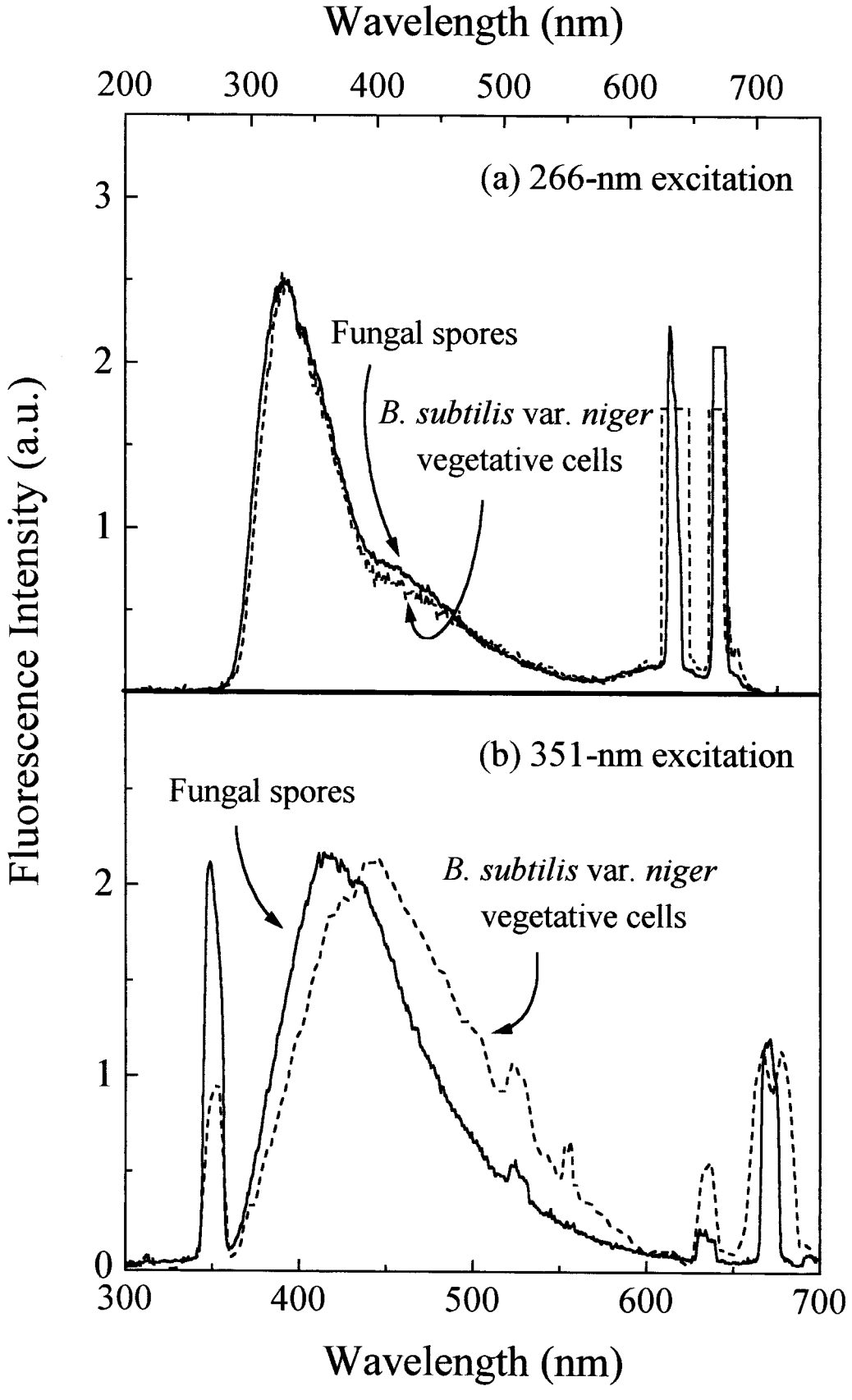

FIG. 11. Fluorescence spectra of a bacteria (*B. subtilis* var. *niger* vegetative cells) and fungal spores. All spectra are averages for 100 nominal 5-μm-diameter particles. For 266-nm excitation (a), the bacteria and fungal spores have almost identical spectral features; whereas for 351-nm excitation (b), the spectra are different, suggesting that multiwavelength excitation of fluorescence can provide more discrimination among biological particles than single-wavelength excitation.

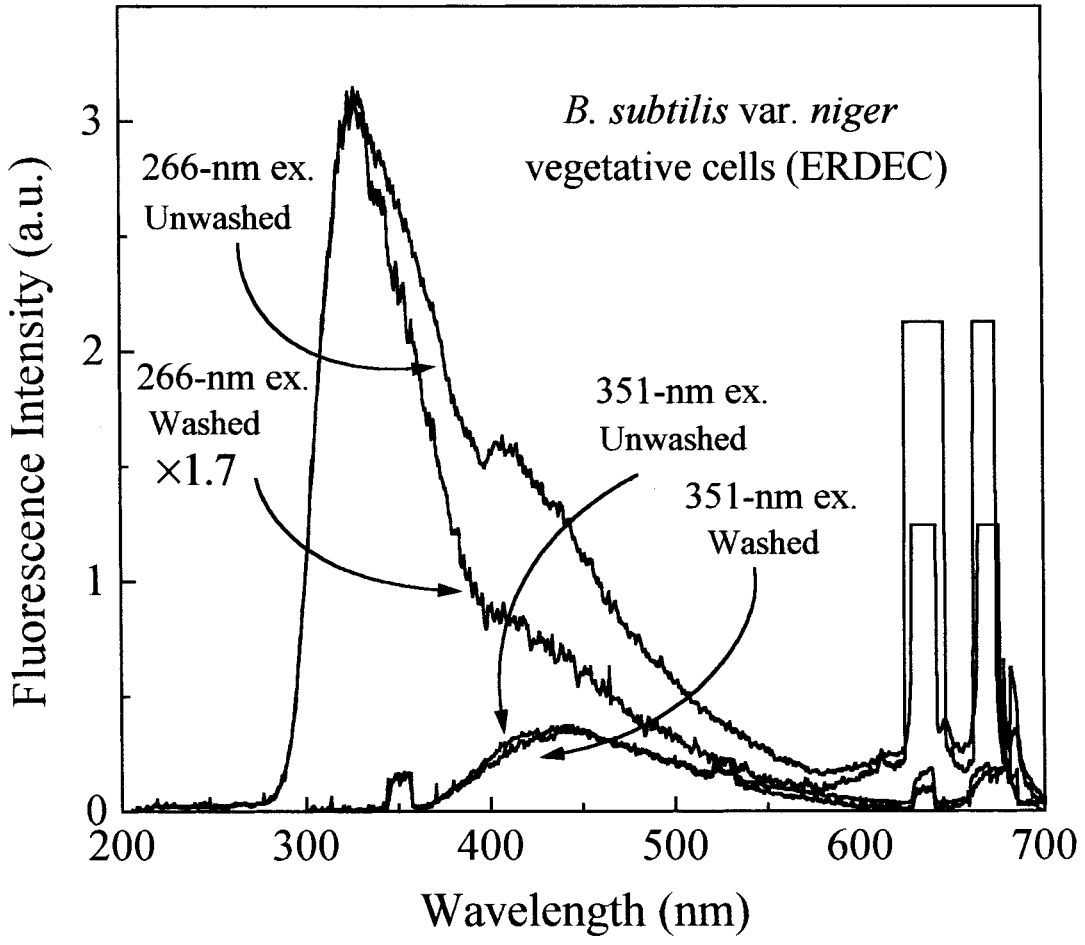

FIG. 12. Fluorescence spectra of an unwashed and washed bacteria *B. subtilis* var. *niger* vegetative cells. All spectra are averages of 100 nominal 5-μm-diameter particles. For 351-nm excitation (b), the washed and unwashed bacteria have similar spectral features; for 266-nm excitation (a), the spectra are different.

gation region was made small to ensure that the particle is examined only when it is in the small focal volume of the high-NA reflecting lens.)

With a more sensitive detector (such as a multianode PMT), and dispersion of the fluorescence into fewer channels (e.g., 32, instead of the present 1000 channels), the SNR may be increased by a factor of 100. With this detector upgrade the sample volume could be increased and the sample rate increased to perhaps 6 l/min.

Conclusions

We have demonstrated an intrinsic-fluorescence-based method for the detection and classification of bioaerosols. Our detection system can capture the UV-excited fluorescence spectra of single, μm-sized bacteria, pollens, and fungal spores as they are carried by a stream of air rapidly through the sample volume. In some of the cases we have studied, the fluorescence spectra allow for differentiation of (1) bacteria from common atmospheric aerosols such as ammonium sulfate, ammonium nitrate, quartz and clay minerals of soil origin, and black carbon; (2) some bacteria from some pollens and some allergens; (3) one species of bacteria prepared in different ways; and (4) washed and unwashed bacteria. We have shown that multiple-wavelength excitation provides an advantage for distinguishing bioaerosols.

Although intrinsic fluorescence by itself cannot be used to specifically identify airborne microorganisms, pollens, or allergens, we expect that single-particle fluorescence spectra along with elastic scattering measurements of each particle will be useful for real-time classification of atmospheric bioaerosols into some as-yet-unknown set of classes. Given the recent availability of triggerable diode-pumped solid-state UV lasers and multianode PMT detectors, it should be possible to develop the fluorescence spectral method into a field-portable instrument. Such an instrument should be able to run continuously without requiring reagents, and without requiring the particles to be collected from the air. The instrument should be able to detect bioaerosols that it has not been presented previously and suggest when to turn on a system for specific identification. The real-time capability

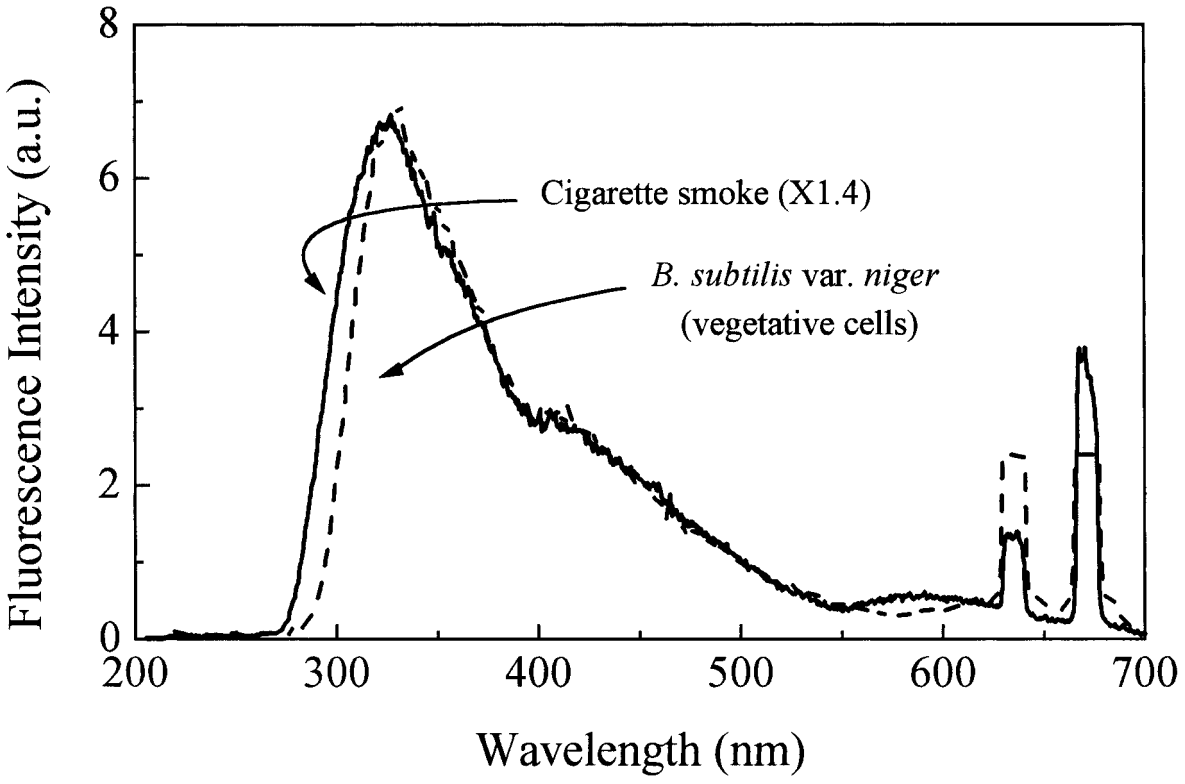

FIG. 13. Fluorescence spectra of side-stream tobacco smoke averaged over 100 laser shots. A lighted cigarette was held within a few centimeters of the apparatus and the smoke drifted into the sample region. There were probably multiple particles within the sample volume during each laser shot. Also shown is a 100-shot average of *B. subtilis* var. *niger* vegetative cells (5-μm-diameter particles) normalized to the peak fluorescence around 330-nm wavelength.

should be useful for studies of intermittent events, bioaerosol dynamics, etc.

Acknowledgments

We thank Burt V. Bronk for guidance on this project.

References

1. Lighthart B, Shaffer, B. Airborne bacteria in the atmospheric surface layer: Temporal distribution above a grass seed field. Appl Environ Microbiol 1995;61:1492–1496.
2. Lighthart B, Stetzenbach LD. Distribution of microbial bioaerosol. In: Lighthart B, Mohr AJ, editors. Atmospheric microbial aerosols. New York: Chapman & Hall; 1994. chap. 4, p 68–98.
3. Matthias-Maser, S, Jaenicke, R. Examination of atmospheric bioaerosol particles with radii greater than 0.2 micrometers. J Aerosol Sci 1994;25:1605–1613.
4. Crook B, Olenchock SA. Industrial workplaces. In: Cox CS, Wathes CM, editors. Bioaerosols handbook. Boca Raton: Lewis; 1995. chap 19.
5. Burge H. Bioaerosols in the residential environment. In: Cox CS, Wathes CM, editors. Bioaerosols handbook. Boca Raton: Lewis; 1995. chap. 21.
6. Custovic A, Fletcher A, Pickering CAC, Francis HC, Green R, Smith A, Chapman M, Woodcock A. Domestic allergens in public places III: House dust mite, cat, dog and cockroach allergens in British hospitals. Clin Exp Allergy 1998;28:53–59.
7. Fincher EL. Aerobiology and hospital sepsis. In Dimmick RL, Akers AB, editors. An introduction to experimental aerobiology. New York: Wiley Interscience; 1969.
8. Zacharisen MC, Kadambi AR, Schlueter DP, Kurup VP, Shack JB, Fox JL, Anderson HA, Fink JN. The spectrum of respiratory disease associated with exposure to metal working fluids. J Occup Environ Med 1998;40:640–647.
9. Brachman PS, Kaufmann AF, Dalldorf FG. Industrial inhalation anthrax. Bacteriol Rev 1966;30:646–659.
10. Kullman GJ, Thorne PS, Waldron PF, Marx JJ, Ault B, Lewis DM, Siegel PD, Olenchock SA, Merchant JA. Organic dust exposures from work in dairy barns. Am Ind Hyg Assoc J 1998;59:403–413.
11. Wathes CM. Bioaerosols in animal houses. In: Cox CS, Wathes CM, editors. Bioaerosols handbook. Boca Raton: Lewis; 1995. chap. 20.
12. Pillai SD, Widmer KW, Dowd SE, Ricke SC. Occurrence of airborne bacteria and pathogen indicators during land application of sewage sludge. Appl Env Microbiol 1996;62:296–299.
13. Marchand G, Lavoie J, Lazure L. Evaluation of bioaerosols in a municipal solid waste recycling and composting plant. J Air and Waste Manage Assoc 1996;45:778–781.
14. Rahkonen P, Ettala M, Laukkanen M, Salkinoja-Salonen M. Airborne microbes and endotoxins in the work environment of two sanitary landfills in Finland. Aerosol Sci Technol 1990;13:505–513.
15. Laitinen S, Nevalainen A, Kotimaa M, Liesivuori J, Martikainen P. Relationship between bacterial counts and endotoxin concentrations in the air of wastewater treatment plants. Appl Environ Microbiol 1992; 58:3774–3776.
16. Stockholm International Peace Research Institute. The problem of chemical and biological weapons. Vol. 1. The rise of CB weapons. Stockholm: Almqvist and Wiksell; 1971. p 111–124.

17. Messelson M, Guillemin J, Hugh-Jones M, Langmuir A, Popova I, Shelokov A, Yampolskaya O. The Sverdlovsk anthrax outbreak of 1979. Science 1994;266:1202–1208.
18. Henderson DA. The looming threat of bioterrorism. Science 1999;283: 1279–1282.
19. U.S. Congress, Office of Technology Assessment. Technologies underlying weapons of mass destruction (OTA-BP-ISC-115). Washington, DC: U. S. Government Printing Office; 1993. p 71–117.
20. Hewish M. On alert against the bio agents: Tactical biological-agent detection approaches reality. Jane's Int Def Rev 1998;31:53–57.
21. Nevalainen A, Pastuszka J, Liebhaber F, Willeke K. Performance of bioaerosol samplers: Collection characteristics and sampler design considerations. Atmos Environ 1992;26A:531–540.
22. Buttner MP, Stetzenbach LD. Monitoring airborne fungal spores in an experimental indoor environment to evaluate sampling methods and the effects of human activity on air sampling. Appl Environ Microbiol 1993;59:219–226.
23. Alvarez AJ, Buttner MP, Toranzos GA, Dvorsky EA, Toro A, Heikes TB, Mertikas-Pifer LE, Stetzenbach LD. Use of solid-phase PCR for enhanced detection of airborne microorganisms. Appl Environ Microbiol 1994;60:374–376.
24. Stewart SL, Grinshpun SA, Willeke K, Terzieva S, Ulevicius V, Donnelly J. Effect of impact stress on microbial recovery on an agar surface. Appl Environ Microbiol 1995;61:1232–1239.
25. Terzieva S, Donnelly J, Ulevicius V, Grinshpun SA, Willeke K, Stelma GN, Brenner KP. Comparison of methods for detection and enumeration of airborne microorganisms collected by liquid impingement. Appl Environ Microbiol 1996;62:2264–2272.
26. Reponen TA, Gazenko SV, Grinshpun SA, Willeke K, Cole EC. Characteristics of airborne actinomycete spores. Appl Environ Microbiol 1998;64:3807–3812.
27. Pinnick RG, Hill SC, Nachman P, Pendleton JD, Fernandez GL, Mayo MW, Bruno JG. Fluorescence particle counter for detecting airborne bacteria and other biological particles. Aerosol Sci Technol 1995;23: 653–664.
28. Hairston PP, Ho J, Quant FR. Design of an instrument for real-time detection of bioaerosols using simultaneous measurement of particle aerodynamic size and intrinsic fluorescence. J Aerosol Sci 1997;28: 471–482.
29. Seaver M, Eversole JD, Hardgrove JJ, Cary WK, Roselle DC. Size and fluorescence measurements for field detection of biological aerosols. Aerosol Sci Tech 1999;30:174–185.
30. Jeys T. MIT Lincoln Lab., Technical Report ESC-TR-97-136; 1998.
31. Hill SC, Pinnick RG, Nachman P, Chen G, Chang RK, Mayo MW, Fernandez GL. Aerosol-fluorescence spectrum analyzer: Real-time measurement of emission spectra of airborne biological particles. Appl Opt 1995;34:7149–7155.
32. Nachman P, Chen G, Pinnick RG, Hill SC, Chang RK, Mayo MW, Fernandez GL. Conditional-sampling spectrograph detection system for fluorescence measurements of individual airborne biological particles. Appl Opt 1996;35:1069–1076.
33. Chen G, Nachman P, Pinnick RG, Hill SC, Chang RK. Conditional-firing aerosol-fluorescence spectrum analyzer for individual airborne particles with pulsed 266-nm ultraviolet laser excitation. Opt Lett 1996; 21:1307–1308.
34. Pinnick RG, Hill SC, Nachman P, Videen G, Chen G, Chang RK. Aerosol fluorescence spectrum analyzer for rapid measurement of single micrometer-sized airborne biological particles. Aerosol Sci. Technol 1998;28:95–104.
35. Pan YL, Holler S, Chang RK, Hill SC, Pinnick RG, Niles S, Bottiger JR. Single shot fluorescence spectra of individual micro-sized bio-aerosols illuminated by a 351 nm or 266 nm laser. Opt Lett 1999;24:116–119.
36. Pan YL, Hill SC, Pinnick RG, Niles S, Holler S, Chang RK, Bottiger JR, Roselle DC, Eversole JD, Seaver M. Fluorescence spectra of individual flowing airborne biological particles measured in real time. Am Ind Hyg Assoc J; submitted.
37. Cheng YS, Barr EB, Fan BJ, Hargis PJ, Rader DJ, O'Hern TJ, Torczynski JR, Tisone GC, Preppernau BL, Young SA, Radloff RJ. Detection of bioaerosols using multiwavelength UV fluorescence spectroscopy. Aerosol Sci Tech 1999;30:186–201.
38. Gieray RL, Reilly PTA, Yang M, Whitten WB, Ramsey JM. Real-time detection of individual airborne bacteria. J Microbiol Meth 1997;29: 191–199.
39. Kishnamurthy T, Ross PL, Rajamani U. Detection of pathogenic and non-pathogenic bacteria by matrix-assisted laser desorption/ionization time-of-flight mass spectrometry. Rapid Commun Mass Spectrom 1996;10:883–888.
40. Arnold RJ, Reilly JP. Fingerprint matching of E-coli strains with matrix-assisted laser desorption ionization time-of-flight mass spectrometry of whole cells using a modified correlation approach. Rapid Commun Mass Spectrom 1998;12:630–636.
41. Easterling ML, Colangelo CM, Scott RA, Amster IJ. Monitoring protein expression in whole bacterial cells with MALDI time-of-flight mass spectrometry. Anal Chem 1998;70:2704–2709.
42. Dai YQ, Li L, Roser DC, Long SR. Detection and identification of low-mass peptides and proteins from solvent suspensions of Escherichia coli by high performance liquid chromatography fractionation and matrix-assisted laser desorption/ionization mass spectrometry. Rapid Commun Mass Spectrom 1999;13:73–78.
43. Snyder AP, Smith PBW, Dworzanski JP, Meuzelaar HLC. Pyrolysis-gas chromatography-mass spectrometry-detection of biological warfare agents. Mass Spectrom Character Microorg 1994;541:62–84.
44. Beverly MB, Basile F, Voorhees KJ, Hadfield TL. A rapid approach for the detection of dipicolinic acid in bacterial spores using pyrolysis mass spectrometry. Rapid Commun Mass Spectrom 1996;10: 455–458.
45. Snyder AP, Thornton SN, Dworzanski JP, Meuzelaar HLC. Detection of the picolinic acid biomarker in Bacillus spores using a potentially field-portable pyrolysis gas chromatography ion mobility spectrometry system. Field Anal Chem Technol 1996;1:49–59.
46. Dworzanski JP, McClennen WH, Cole PA, Thornton SN, Meuzelaar HLC, Arnold NS, Snyder AP. Field-portable automated pyrolysis-GC/IMS system for rapid biomarker detection in aerosols: A feasibility study. Field Anal Chem Technol 1997;1:295–305.
47. Murrell WG. Chemical composition of spores and spore structures. In: Gould GW, Hurst A, editors. The Bacterial Spore. New York: Academic; 1969. p 218–231 and Table III.
48. Setlow P. Germination and outgrowth. In: Hurst A, Gould GW, editors. The bacterial spore. New York: Academic; 1971. vol 2, p 214–217.
49. Chance B. Spectrophotometric and kinetic studies of flavoproteins in tissues, cell suspensions, mitochondria and their fragments. In Slater EC, editors. Flavins and flavoproteins. New York: Elsevier; 1996. p 496–510.
50. Lakowicz JR. Principles of fluorescence spectroscopy. New York: Plenum; 1983. p 341.
51. Aubin JE. Autofluorescence of viable cultured mammalian cells. J Histochem Cytochem 1979;27:36–43.
52. Benson RC, Meyer RA, Zaruba ME, McKhann GM. Cellular autofluorescence: Is it due to flavins? J Histochem Cytochem 1979;27:44–48.
53. Seaver M, Roselle DC, Pinto JF, Eversole JD. Absolute emission spectra from Bacillus subtilis and Escherichia coli vegetative cells in solution. Appl Opt 1998;37:5344–5347.
54. A two-lens system with f/4 collection was used.
55. We used a flash-lamp-pumped, frequency-quadrupled Nd:YAG laser having a non-Gaussian spatial profile, and significant shot-to-shot variations in intensity.
56. Bottiger JR, Deluca PJ, Stuebing EW, VanReenen DR. An ink jet aerosol generator. J Aerosol Sci 1998;29(suppl 1), s965–966.
57. The Q-switched UV laser is either the 266-nm, fourth harmonic of a Nd:YAG laser [30- or 70-ns pulse duration (Spectra Physics models X-30 or Y-70)], or the 351-nm, third-harmonic of a Nd:YLF laser [120-ns pulse duration (Quantronix)]. The Q-switched laser fires within about 3 μs of the trigger pulse, during which time the particle travels (about 10 m/s) less than 40 μm. This vertical displacement is compen-

sated for by a small vertical displacement of the focal volume of the two diode-laser beams from the UV laser beam (which is focused to the focal point of the reflecting objective).
58. The ICCD camera (Princeton Instruments) is placed at the exit port of the spectrograph (Acton model SP-150 with 300 groove/mm grating blazed at 500 nm, numerical aperture 0.125, input slit width 1 mm). The ICCD detector's image intensifier acts as a fast shutter, opening when the targeted particle is illuminated by the UV laser. A long-pass filter is placed in front of the spectrograph to block elastically scattered light and to pass the fluorescence.
59. To estimate these fractions, the colony-forming units of bacteria and fungi were measured, and the masses were estimated, assuming spherical 1-μm-diameter bacteria at densities of 1 g/cm^3.
60. Sidestream cigarette smoke has been measured[61] to have a log-normal size distribution with number concentration $\approx 3 \times 10^{10}$ cm^{-3}, geometric mean diameter ≈ 0.18 μm, and log-normal standard deviation ≈ 0.4. Thus we would expect the ≈ 100 particles to occupy a spherical sample volume with 10-μm radius.
61. Okada T, Matsunuma K. Determination of particle-size distribution and concentration of cigarette smoke by a light-scattering method. J Colloid Interface Sci 1974;48:461–469.
62. Faris GW, Copeland RA, Mortelmens K, Bronk BV. Spectrally resolved absolute fluorescence cross sections for bacillus spores. Appl Opt 1997;36:958–967.
63. Gelbachs and Birnbaum (Ref. 64) used the 488-nm line of an argon-ion laser to excite fluorescence from atmospheric aerosols. They spectrally dispersed the fluorescence into four large bands, but were unable to obtain detailed spectra or single particle spectra. They noted that if "one type of aerosol predominates, such as cigarette smoke or pollen, a low resolution spectrum," may be adequate. They also suggested that such an instrument may be useful for detecting and identifying aerosol emissions (e.g., fly ash (Ref. 65)) from stacks.
64. Gelbwachs J, and Birnbaum M. Fluorescence of a atmospheric aerosols and lidar implications. Appl Opt 1973;12:2442–2447.
65. Birnbaum M. Laser-excited fluorescence techniques in air pollution monitoring. In: Wehry EL, editor. Modern Fluorescence Spectroscopy, Vol. 1. New York: Plenum; 1976. Chapter 5.
66. Nakamura S, Fasol G. The blue green diode. Berlin: Springer; 1997.